Diffraction anomalous fine structure of forbidden Bragg reflections: charge localization and structure of the octahedral site in magnetite

H. Renevier,[a,b] Y. Joly,[a] J. García,[c] G. Subías,[c] M.G. Proietti,[a,b] J. L. Hodeau,[b] J. Blasco,[b]

[a]Laboratoire de Cristallographie, CNRS, BP. 166, F38042 Grenoble Cedex 9,France, [b]Université Joseph Fourier, BP 53, F-38041, Grenoble Cedex 09, France, [c]Instituto de Ciencia de Materiales de Aragón. Consejo Superior de Investigaciones Científicas y Universidad de Zaragoza, 50009 Zaragoza, Spain.
E-mail: renevier@polycnrs-gre.fr

Resonant X ray scattering has been used to investigate charge localization on the octahedral iron atoms in magnetite below and above the Verwey temperature. We have measured the DAFS spectra of the 002 and 006 "forbidden" Bragg reflections permitted by the anisotropy of the iron anomalous scattering factor. We performed ab initio calculations which are in fair agreement with the experiment in the near edge region and demonstrate the sensitivity of the DAFS spectra to tiny structural and electronic changes. No change is observed, in the energy and azimuthal dependences, when the sample is cooled down below the Verwey temperature. Charge ordering can be definitely excluded and different charge localisation schemes discarded. Ab initio simulations, performed by using the refined crystallographic structure proposed for the room temperature phase, do not show a good agreement with the experiment in the extended region of the DAFS spectrum. This point is being investigated.

Keywords: Diffraction Anomalous Fine Structure magnetite charge ordering

1. Introduction

Mixed valence transition metal oxides exhibit many interesting properties such as superconductivity, colossal magnetoresistance and metal insulator phase transitions. Generally, the description of the electronic state of these compounds is made on the basis of the ionic model and it implies the spatial or temporal charge localization on the transition metal atoms (Goodenough, 1963). Magnetite (Fe_3O_4) is the oldest known magnetic material and the original Néel ferrimagnet (T_N = 851 K) (Néel, 1948). It can be considered as the prototype of the inverse spinel ferrite (Brabers, 1995). At room temperature magnetite crystallizes with the cubic space group Fd $\bar{3}$ m ; the tetrahedral A sites contain one third of the iron ions as Fe^{3+} and the octahedral B sites contain the remaining Fe ions with equal numbers of Fe^{3+} and Fe^{2+} (Fleet, 1981). Below 851K magnetite is ferrimagnetic with A sites moments aligned antiparallel to the B-sites moments. Above the so-called Verwey temperature (Tv $\approx$ 125K), both NMR and Mossbauer spectroscopies detect only one kind of iron cations on the B sites indicating that the charge carriers are delocalised (note that the characteristic time of NMR is 10^{-8}s). Below Tv, the crystal symmetry is lowered to monoclinic and the electric conductivity drops by two order of magnitude. Refinement of the crystal structure could be made only in the orthorhombic system (Izumi *et al.,* 1982) and the very complex crystallographic distortions are not yet fully understood. The distortions were described as the result of few phonon condensation. Although the B iron local environment is slightly distorted the mean Fe-O distance is very close to the Fe-O distance in the cubic structure, suggesting an absence of charge localisation. Recent NMR results (Novak et *al.*, 2000) are in accordance with the monoclinic symmetry, more important, only one relaxation time was found for iron on the B site thus suggesting that no charge localization occurs below Tv. Magnetite was the first material in which a charge ordering transition was proposed to explain the metal insulator phase transition. The classical mechanism to describe this transition states that the distribution of octahedral Fe^{3+} and Fe^{2+} ions changes from dynamical disorder to long range order by lowering the temperature. Verwey stated that charge localization could manifest with alternating Fe^{3+} and Fe^{2+} in the [001] direction leading to superlattice reflections like the 002 (Verwey, 1939). Nevertheless, this point has not yet been demonstrated. We report the observation of the 002 and 006 forbidden reflections, below and above the Verwey transition (125K), by means of X-ray resonant scattering at the iron K-edge. Note that if the scattering is isotropic (Thomson scattering), the 002 and 006 reflections are forbidden above Tv because of the d-glide plane of the space group Fd $\bar{3}$ m.

2. Resonant scattering

Atomic resonant scattering $f'+if''$ (or atomic anomalous scattering) results from virtual multipole transitions when the incoming x-ray beam energy is close to an absorption threshold. Considering only the dipole and quadrupole terms :

$$f'+if'' = (\hbar\omega)^2 \times \sum_{f,g} \frac{\left\langle \psi_g \left| \vec{\varepsilon}_s.\vec{r} - \frac{i}{2}\vec{\varepsilon}_s.\vec{r}\vec{k}_s.\vec{r} \right| \psi_f \right\rangle \left\langle \psi_f \left| \vec{\varepsilon}_e.\vec{r} + \frac{i}{2}\vec{\varepsilon}_e.\vec{r}\vec{k}_e.\vec{r} \right| \psi_g \right\rangle}{\hbar\omega - E_f + E_g + i\frac{\Gamma}{2}} \quad (1)$$

where f and g represent the final and initial (1s) states, $\vec{\varepsilon}_e, \vec{k}_e, \vec{\varepsilon}_s, \vec{k}_s$ the polarization and wave numbers of the incoming and outgoing x-ray beams. Expression (1) shows that the dipole transition depends on $\vec{\varepsilon}_e, \vec{\varepsilon}_s$ and quadrupole one on $\vec{\varepsilon}_e, \vec{k}_e, \vec{\varepsilon}_s, \vec{k}_s$. Thomson scattering (isotropic) only depends on the scattering vector $\vec{Q}$. Also important is the energy level of the initial state E_g. It is well known that atomic resonant scattering factors $f'+if''$ are very sensitive to charge localization because the 1s energy of the initial state (E_g) as well as the nearest neighbour distances, strongly depend on the charge localization in the 3d orbitals. For instance an increase of the formal valence results in a shift of the resonant energy toward high values due to the decrease of both the distances and the 1s energy. Expression (1) also tells us that the symmetry of the local environment may give rise to an anisotropy of the resonant scattering (Anisotropy of the Tensor of Suceptibility, ATS). This phenomenon, known as the Templeton's effect was extensively studied (Templeton et *al*. 1980, Dmitrienko, 1983), it is responsible for the appearance of forbidden reflections reported in this study. A DAFS experiment consists in measuring the scattered intensity which is proportional to the modulus square of the structure factor, as function of energy (Cross et *al.*, 2000).

3. Experimental results

Experiments were performed at the beamline BM2-D2AM at the ESRF (Ferrer et *al.*, 1998). A single crystal of magnetite was grown by the floating zone method using halogen lamps. The crystal was oriented and polished to obtain a flat clean (100) surface. The incident beam was monochromatized by Si(111) double crystals. The energy resolution was about 0.5 eV. The incident polarization vector was perpendicular to the diffraction plane (σ incident

 © 2001 International Union of Crystallography • Printed in Great Britain – all rights reserved

geometry) and σ–σ polarisation analysis of the scattered beam was performed using an MgO (222) crystal analyzer with a scattering angle of 45.811 º at the iron K edge (7.112 keV). The energy dependence of the intensity of the 002 and 006 reflections, with the x-ray beam polarisation along the [110] direction, at 20 K and at room temperature is shown in fig. 1 together with the fluorescence spectrum. As it can be observed, the energy dependence of the scattered intensity is the same for both temperatures. No detectable intensity below the absorption edge was observed. Three main features can be distinguished on the spectra as a function of the energy : a) a resonance at the pre-edge peak energy of the fluorescence spectrum corresponding to a virtual excitation-de-excitation through dipolar-quadrupolar channels at the tetrahedral iron atom (A site) b) a strong resonance at the 1s-4p energy transition, due to the anisotropy of the dipolar scattering factor of the trigonal (-3m) octahedral iron atoms (B site) c) the extended part above the edge that has the same origin as the main resonance and shows an oscillatory behaviour as a function of the energy.

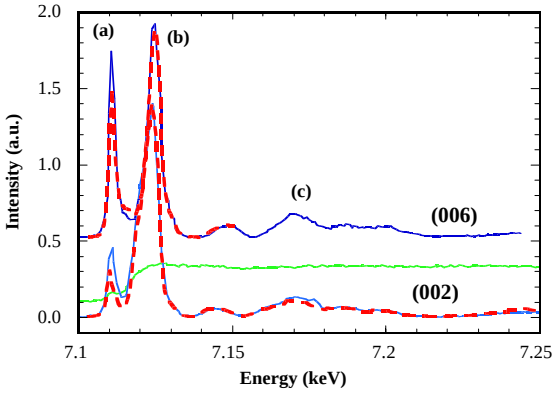

Figure 1
Intensity versus photon energy of 002 and 006 forbidden reflections with the incident light polarization vector parallel to the [110] crystallographic direction. The spectra have been recorded at 20K (dashed line) and room temperature (solid line). The fluorescence spectrum is also shown (gray curve). The fluorescence background was subtracted but the spectra are not corrected for self-absorption

Table 1
Multipole contributions of the two iron sites to the resonant scattering

Site symmetry	Dipole/Dipole	Dipole/Quadr.	Quadr./Quadr.
Oh (-3m)	1	0	$cos^4(2\theta)$
Th (-43m)	0	$cos^2(2\theta)$	0

Table 1 shows the multipole contributions of the two iron sites to the resonant scattering. The symmetry of the tetrahedral site being cubic no dipole-dipole contribution is expected, but the dipole-quadrupole transition is not forbidden (Templeton et *al.*, 1994). The centrosymmetry of the octahedral site preclude a dipole-quadrupole contribution. Simulation of the spectra were performed using the program FDMNES (Joly, 1999) which takes into account the polarisation and wave vector of the incoming and outgoing x-ray beams, as well as charge localization and shift in energy due to different oxidation states and site symmetry. The calculations were done using the crystallographic structure at room temperature with a valence a 2.5+ ($3d^{5.5}$) for all iron in the octahedral sites. Figure 2 shows the best Full Multiple Scattering (FMS) calculation (Green's formalism) obtained with a cluster size of radius 3.5Å, i.e. including up to the third shell. Increasing the size of the cluster does not improve the agreement with the experimental curve. Analysis of EXAFS data is underway for comparison. As can been seen in figure 2 simulations agree quite well in the near edge region but not above 100eV.

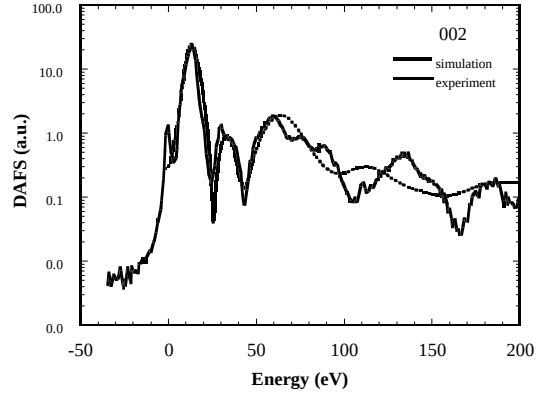

Figure 2
Full Multiple Scattering calculation with FDMNES of the 002 DAFS spectrum. Only the dipolar contribution is shown.

The crystallographic structure may be not exactly the correct one or the simulation fails to reproduce the data that corresponds in this region to a very tiny anisotropy difference. Investigation of that point is underway. The experimental curves were corrected for absorption using an absorption spectrum of a powder recorded in transmission mode. It should be noted that except at the edge, DAFS oscillations at "forbidden" reflection are barely affected by self absorption, even in the case of a bulk sample with a high concentration of anomalous atoms, such as magnetite. As a matter of fact there is no contribution of the Thomson scattering to the absorption effect and the relative absorption correction is small in the extended region. Inelastic losses were taken into account with the Sea and Dench formula and a 0.5eV core hole broadening was used. The dependence of the experimental dipole contribution (a and b features on figure 1) as a function of the azimuthal angle ψ follows as a whole, the theoretical azimuthal dependence calculated by assuming that all iron on the B sites have identical local environment and valence. In that case, the azimuthal dependence of the 002 diffraction spectrum can be obtained as follow. Iron on the B sites sits on a centre of inversion and a 3-fold axis. The dipole atomic scattering factor can be written in the crystallographic frame :

$$f = \begin{pmatrix} f_{xx} & f_{xy} & f_{xy} \\ f_{xy} & f_{xx} & f_{xy} \\ f_{xy} & f_{xy} & f_{xx} \end{pmatrix} \text{ and } F_{002} = 16i \begin{pmatrix} 0 & f_{xy} & 0 \\ f_{xy} & 0 & 0 \\ 0 & 0 & 0 \end{pmatrix}$$, where F is the structure factor obtained by summing over the B sites. The scattered intensity is proportional to $\left|\vec{\varepsilon}_s F \vec{\varepsilon}_e\right|^2$. For the 002 reflection (the same holds true for the 006) the intensity in the σ-π and σ-σ channels are $I_{002}^{\sigma\pi} = \left|16 f_{xy}\right|^2 cos^2(2\psi) sin^2(\theta)$ and $I_{002}^{\sigma\sigma} = \left|16 f_{xy}\right|^2 sin^2(2\psi)$ respectively. From that point on, one can demonstrate that $f_{xy} = 1/3(f_{//} - f_{\perp})$ where // and ⊥ refer to the scattering in the trigonal axis frame. The anomalous scattering factors can be written $f'_{//,\perp} = \Delta f'_{0Fe}(1 + \chi'_{//,\perp})$ and

$f''_{//,\perp} = \Delta f''_{0Fe}(1+\chi''_{//,\perp})$, this allows to expand $\left|f_{xy}\right|^2$ over scattering paths in the extended region :

$$\left|f_{xy}\right|^2 = (\Delta f''_{0Fe})\left[\sum_{\Gamma}\Delta A_{\Gamma}^2 + \sum_{\Gamma>\Gamma'} 2\Delta A_{\Gamma}\Delta A_{\Gamma'}\cos\left[2k(r_{\Gamma}-r_{\Gamma'})+(\delta_{\Gamma}-\delta_{\Gamma'})\right]\right] \quad (2)$$

where $\Delta f''_{0Fe}$ is the contribution to the Fe scattering factor of the resonant electronic transition alone, r_{Γ} ($r_{\Gamma'}$) the distances from the central atom, δ_{Γ} ($\delta_{\Gamma'}$) the atomic phase shifts, $\Delta A_{\Gamma} = A_{//} - A_{\perp}$ and Γ a scattering path.

Expression (2) shows that the oscillatory signal comes from the addition of cosine terms whose frequencies are twice the difference between different coordination shells. Indeed, simulations show that barely any contribution is obtained in the extended part with only one shell consisting of an oxygen octahedron slightly stretched along the [111] direction (rhombohedral distortions). Expression (2) also shows the sensitivity of the resonant scattering not only to small structural changes but also to charge localization that modifies the phase shift differences. For instance, simulations show that an increase of the rhombohedral distortion of the octahedra, that would lead to an increase of the Fe-O distance of 0.002Å, can be clearly observed. This is the first time that anisotropy of the atomic scattering factor in the extended part is reported and a coherent explanation of its origin is given (Garcia et *al*., 2000).

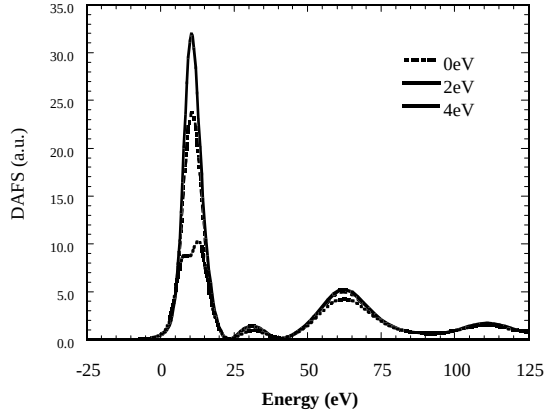

Figure 3
Simulations of random charge disproportionations obtained by averaging atomic scattering factors with chemical shifts of 0, 2 and 4eV. Except the chemical shift all parameters are the same as those used for the calculations presented on figure 2.

The most important experimental result is shown in figure 1 : the spectra (b and c features) above and below Tv are identical.

The azimuthal dependences (not shown) are also identical. Only a slight decrease of the intensity of the pre-edge peak (feature (a)) is observable, that is probably the result of a slight deformation of the tetrahedral sites at low temperature (Izumi et *al*., 1982). As a matter of fact, it is well established that the main difference between anomalous scattering factors with different oxidation states is the chemical shift. In the case of Fe^{3+} and Fe^{2+}, the chemical shift is in between 3 and 5 eV (edge shifts), so charge fluctuation in time scale larger than the interaction time for the virtual process involved (10^{-16} sec), will modify the atomic scattering factor and consequently the diffraction intensity. As an example simulations of random charge disproportionations obtained by averaging atomic scattering factors with chemical shifts of 0, 2 and 4eV are shown on figure 3. A value of 2 eV already gives a detectable change. It is important to note the change in the relative intensities of the peaks. For a shift of 4eV, the main peak starts to split, leading also to the conclusion that a random charge disproportionation at a given temperature, that would lead to a chemical shift greater than 4eV, can be discarded. Simulations also show that charge ordering along the [001] direction can clearly be ruled out. In that case, the chemical shift would change the spectrum not only in the near edge region but also in the extended part. Moreover, in the near edge region, XANES spectra of different cations as Fe^{2+} and Fe^{3+} are quite different from each other, leading to a constant intensity that we did not observe.

4. Conclusion

We have shown that : a) the 00*l* ATS reflections are very sensitive to tiny distortions, displacements and electronic changes at the B site b) no change of energy and azimuthal dependences is observed when cooling down the sample below the Verwey temperature. One can definitely discard different charge localization schemes above and below Tv. There is no evidence of charge ordering or random charge localization at the octahedral sites. As a consequence, the metal-insulator transition is likely produced by the crystallographic distortion rather than charge localization. Further simulations are in progress to understand the pre-edge peak intensity change. On the other hand more work should be done to find the structural phase transition that leaves the local structure of the B sites unchanged.

This work was supported by the Spanish CICyT project nº MAT96-0491 and the LEA-MANES project. The authors warmly thank C.R. Natoli for fruitful discussions and ESRF for beam time granting.

References

Brabers V. A. M., in Handbook of Magnetic Materials, edited by K. H. J. Buschow (Elsevier Science, Amsterdam,1995) vol 8, p 199.
Ferrer J.L., Simon J. P., Bérar J. F., Caillot B., Fanchon E., Kaikati O., Arnaud S., Guidoti M., Pirocchi M., Roth M., (1998), J. Synchrotron Rad. **5**, 972.
Fleet, M.E. (1981), Acta Cryst., B37, 917-920.
Izumi, M., Koetzle, T.F., Shirane, G. Chikazumi, S., Matsui, Todo, S. (1982), Acta Cryst., B58, 2121-2133.
Garcia, J., Subias, G., Proietti, M. G., Renevier, H., Joly, Y., Hodeau, J. L., Blasco, J., Sanchez M. C., Bérar, J. F., (2000), Phys. Rev. Lett., 572.
Goodenough J. B., Magnetism and Chemical Bond, Interscience, New York 1963.
Joly, Y., (1999), Phys. Rev. B., submitted. FDMNES code : http://www-cristallo.polycnrs-gre.fr
Néel L., (1948), Ann. Phys. (Leipzig) **3**, 137.
Novák, P., Stépànkova, H., Englich, J., Kohout, J., Brabers, V. A. M., (2000). Phys. Rev. B **61**, 1256-1260.
Templeton D. H. and Templeton L. K. (1980) Acta Cryst **A36**, 436, Dmitrienko V. E., (1983), Acta Cryst. **A39**, 29; Petcov A, Kierfel A., Fisher, K., Acta Cryst. **A46**, (1990), 754. Kirfel A, (1994) in Resonant Anomalous X-Ray Scattering, edited by G. Materlik, C. J. Sparks and K. Fisher. Elsevier Science B.V. Amsterdam.
Templeton, D. H, Templeton, L.K., (1994), Phys. Rev. B. **49**, 14850.
Cross, J., (2001), in Proceedings of the XAFS 11 Conference, AKO, J. Synchrotron Rad. See also the DAFS bibliography at http://cars9.uchicago.edu/~newville/dafs/bib/dafs.html
Verwey E. J. W., (1939), Nature (London) **144,** 327.